

Spectra of ultrabroadband squeezed pulses and the finite-time Unruh-Davies effect

T.L.M. Guedes,^{1,*} M. Kizmann,¹ D.V. Seletskiy,^{1,2} A. Leitenstorfer,¹ Guido Burkard,¹ and A.S. Moskalenko^{1,†}

¹*Department of Physics and Center for Applied Photonics,
University of Konstanz, D-78457 Konstanz, Germany*

²*Department of Engineering Physics, Polytechnique Montréal, H3T 1J4, Canada*

(Dated: October 22, 2018)

We study spectral properties of quantum radiation of ultimately short duration. In particular, we introduce a continuous multimode squeezing operator for the description of subcycle pulses of entangled photons generated by a coherent-field driving in a thin nonlinear crystal with second order susceptibility. We find the ultrabroadband spectra of the emitted quantum radiation perturbatively in the strength of the driving field. These spectra can be related to the spectra expected in an Unruh-Davies experiment with a finite time of acceleration. In the time domain, we describe the corresponding behavior of the normally ordered electric field variance.

PACS numbers: 42.50.Dv, 42.50.Lc, 42.65.Re, 04.62.+v

Introduction.—In quantum optics, parametric down-conversion (PDC) in nonlinear crystals (NXs) has been routinely used to generate pairs of monochromatic entangled photons [1, 2]. The so obtained squeezed states of light have found applications in a broad range of areas like gravitational wave detection [3, 4], quantum communication systems [5–7] and precision measurements [8, 9]. The active interest in squeezed states can be mainly related to the fact that the variance of a given phase space quadrature (a quantum-optical analogue of a canonical variable) is lower for a squeezed state than for a coherent state, including the vacuum state itself. In order to fulfill Heisenberg’s uncertainty principle the variance of the conjugate quadrature exhibits the opposite behavior.

In recent years, theoretical and experimental efforts have been made to describe and generate multimode squeezed states [10–15]. Although they have already been experimentally realized by a number of groups [12, 15], most of the achievements so far are limited to squeezed states with relatively narrow spectra, where the central frequency approximation is still valid. New developments in ultra-stable few-cycle laser sources and advanced detection techniques have paved the way for the generation of few-cycle pulses of mid-infrared (MIR) squeezed light and the electro-optic detection of their electric field statistics with subcycle temporal resolution [16–18]. The subcycle features in the noise patterns of the generated quantum fields are due to the spatio-temporal modulation of the refractive index of the NX induced by the driving field [18]. This is analogous to a time-dependent metric for the space-time occupied by the electric field, which leads to photon creation in the perspective of a moving observer [19].

The spectral properties of ultrabroadband squeezed states are also of particular interest because they can elucidate connections between quantum gravitational effects and their table-top optical analogues. A characteristic example is the Unruh-Davies effect [20, 21], according to which an observer in a non-inertial reference frame,

moving with constant acceleration in the vacuum of an inertial reference frame, should detect thermal radiation. This phenomenon is closely related to the Hawking radiation believed to be emitted at the horizon of black holes [22].

The direct observation of these predictions is at the present time infeasible due to technological limitations, and thus optical counterparts were proposed [23–28] as a means of studying the physics behind such effects. However, little attention has been paid to the effects of the unavoidably finite (and often short) duration of the effective acceleration experienced by either the light or the detector in the suggested experiments.

In this Letter, we first introduce a squeezing operator capable of describing the multimode states generated in a very thin NX with $\chi^{(2)}$ nonlinearity when a coherent ultrashort driving pulse is applied. The relevant experimental setup is schematically shown in Fig. 1(a). Due to the minute thickness of the crystal, phase matching can be assumed perfect. The driving pulse induces a nonlinear mixing cascade, with the PDC acting as a seed for the subsequent frequency conversion processes. The superposition of these forms the structure of the emitted quantum field. Next, we study its spectral properties and confirm the ultrabroadband character of the generated pulses of squeezed light. Moreover, perturbative calculation of the time-dependent variance of the electric field operator links our work with related experimental results on subcycle-resolved sampling of the electric field statistics of quantum-optical states [16–18]. Finally, we make a comparison of the obtained spectra for ultrabroadband squeezed pulses and thermal radiation, aiming to elucidate connections with the Unruh-Davies radiation. It turns out that the limited lifetime of the refractive index perturbation in the crystal results in spectra with exponentially decaying high-frequency tails, which depend on the duration of the perturbation. This result can be related to the diamond temperature [29, 30] derived for the Unruh-Davies effect when the observer follows an ac-

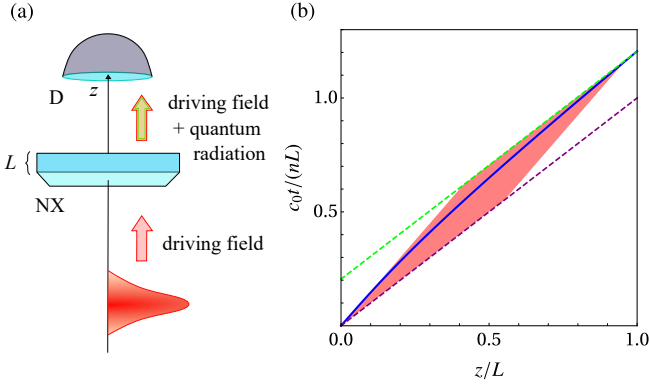


FIG. 1. (a) General sketch of the proposed experimental setup. The classical driving field propagates through a $\chi^{(2)}$ nonlinear crystal (NX) of small thickness L and unperturbed refractive index n , generating ultrabroadband squeezed quantum light. The outgoing light is registered by the detector D. (b) World line of a plane wave mode of the quantum electric field within the NX with refractive index modulated by a half-cycle pulse (HCP). The trajectory (blue) is given by Eq. (9) with $C_1 = 0$, $\alpha/n^2 = 0.49$ and $n\xi = 12$. The dotted purple straight line indicates the trajectory of light in the absence of nonlinear effects. After the acceleration has mostly ceased, the world line approaches the dotted green line parallel to the purple one. The process of acceleration is confined to a diamond-like space-time zone (light red parallelogram) of dimensions defined by the duration of the driving transient.

celerated trajectory during a finite time interval. In our treatment, however, it is the observed incoming vacuum state that undergoes an effective acceleration within a certain space-time zone. This is illustrated in Fig. 1(b) for a plane wave mode of a quantum field that simultaneously enters the crystal with the peak of the driving field.

Squeezing operator.—Considering previously proposed expressions for a multimode squeezing operator [11, 31] and using the convention $\hat{a}(-\omega) = \hat{a}^\dagger(\omega)$ ($\omega \in \mathbb{R}$) connecting creation and annihilation operators for positive and negative frequencies [32], we introduce the following ansatz for the form of the (continuous) multimode squeezing operator:

$$\hat{S}[\xi] = \exp \left\{ \frac{1}{2} \left[\xi_{\omega_1, \omega_2}^* \hat{a}(\omega_1) \hat{a}(\omega_2) - \xi_{\omega_1, \omega_2} \hat{a}^\dagger(\omega_1) \hat{a}^\dagger(\omega_2) \right] \right\}. \quad (1)$$

Here, we employed a generalized Einstein's convention meaning that product terms are integrated from $-\infty$ to ∞ over all continuous variables with reoccurring integer indices. For the unitarity of the squeezing operator the frequency-dependent squeezing parameter $\xi_{\omega, \omega'}$ must satisfy $\xi_{\omega, \omega'} = \xi_{\omega', \omega}$, since then $\hat{S}^\dagger[\xi] = \hat{S}[-\xi]$ and hence $\hat{S}[\xi]^\dagger \hat{S}[\xi] = 1$. Rewriting Eq. (1) solely in terms of positive frequencies would lead to four terms in the integrand of the exponent. Two of them correspond to parametric down-conversion (PDC), while the remaining two corre-

spond to frequency-conversion.

In order to calculate expectation values of operators for the states generated by (1), let us investigate how \hat{a} and \hat{a}^\dagger transform under \hat{S} . We utilize a common procedure in quantum optics [33] by introducing an auxiliary operator $\hat{G}[\tilde{z}; \xi] = \hat{S}^{\tilde{z}}[\xi]$ for $\tilde{z} \in [0, 1]$, which commutes with $\hat{S}[\xi]$. We then define $\hat{a}(\tilde{z}; \omega) = \hat{G}^\dagger[\tilde{z}; \xi] \hat{a}(\omega) \hat{G}[\tilde{z}; \xi]$ so that $\hat{a}(0; \omega) = \hat{a}(\omega)$ and $\hat{a}(1; \omega) = \hat{a}'(\omega) = \hat{S}^\dagger[\xi] \hat{a}(\omega) \hat{S}[\xi]$. The commutator can be calculated using $[\hat{a}(\omega), \hat{a}(\omega')] = \delta(\omega + \omega') [\text{sign}(\omega) - \text{sign}(\omega')]/2$ for any $\omega, \omega' \in \mathbb{R}$. Differentiating $\hat{a}(\tilde{z}; \omega)$ with respect to \tilde{z} and inserting the expression for $\hat{G}[\tilde{z}; \xi]$ leads to

$$\begin{aligned} \frac{\partial \hat{a}(\tilde{z}; \omega)}{\partial \tilde{z}} &= \Xi_{\omega, \omega_1} \hat{a}(\tilde{z}; \omega_1), \\ \Xi_{\omega, \omega'} &= -\text{sign}(\omega) (\xi_{\omega, -\omega'} - \xi_{\omega', -\omega}^*). \end{aligned} \quad (2)$$

This integro-differential operator equation can be solved perturbatively expanding in Ξ , resulting in the Bogoliubov transformation

$$\hat{a}(\tilde{z}; \omega) = U_{\omega, \omega_1}(\tilde{z}) \hat{a}(\omega_1), \quad (3)$$

$$U_{\omega, \omega'}(\tilde{z}) = \delta(\omega - \omega') + \tilde{z} \Xi_{\omega, \omega'} + \frac{\tilde{z}^2}{2!} \Xi_{\omega, \omega_1} \Xi_{\omega_1, \omega'} + \dots$$

Eq. (3) assures the relation $\hat{a}(\tilde{z}; -\omega) = \hat{a}^\dagger(\tilde{z}; \omega)$.

Spectra.—The squeezing process depends on the buildup of electric fields within the NX, which determine the squeezing parameter in Eq. (3). Such interacting fields $\hat{E}(z, t)$ propagating along the z -axis in the crystal [see Fig. 1(a)] can be expressed in terms of plane waves confined to a certain transverse area [17], $\hat{E}(z, t) = \hat{E}(z, \omega_1) \exp[-i\omega_1(t - nz/c_0)]$. Here c_0 is the speed of light in free space and n is the unperturbed refractive index of the medium. It can be found [18] that due to the $\chi^{(2)}$ interaction process a coherent mid-infrared (MIR) driving field of sufficiently large amplitude $E_{\text{MIR}} = \langle \hat{E}_{\text{MIR}} \rangle$ with respect to the amplitude of vacuum fluctuations [16] modulates the quantum contribution $\delta \hat{E} \equiv \hat{E} - E_{\text{MIR}}$ as

$$\frac{\partial \delta \hat{E}(z; \omega)}{\partial z} = \frac{id\omega}{nc_0} E_{\text{MIR}}^*(z; \omega_1 - \omega) \delta \hat{E}(z; \omega_1). \quad (4)$$

Here d is the effective nonlinear coefficient of the NX, considered to be dispersionless in the relevant frequency range.

We can change now the variable $z \rightarrow \tilde{z} = z/L$ in Eq. (4) and use [34] $\delta \hat{E}(z; \omega) = i \text{sign}(\omega) \sqrt{\frac{\hbar|\omega|}{4\pi\epsilon_0 c_0 n A}} \hat{a}(z; \omega)$, where A is the normalization area, \hbar is the reduced Planck constant and ϵ_0 is the vacuum permittivity. If we consider that $E_{\text{MIR}}(z; \omega)$ does not change appreciably as a function of z , comparison of the result with Eq. (2) gives

$$\Xi_{\omega, \omega'} = iC \text{sign}(\omega') \sqrt{|\omega\omega'|} E_{\text{MIR}}(\omega - \omega'), \quad (5)$$

where $C = dL/(nc_0)$. Similar expressions have been used to describe independent frequency-conversion and

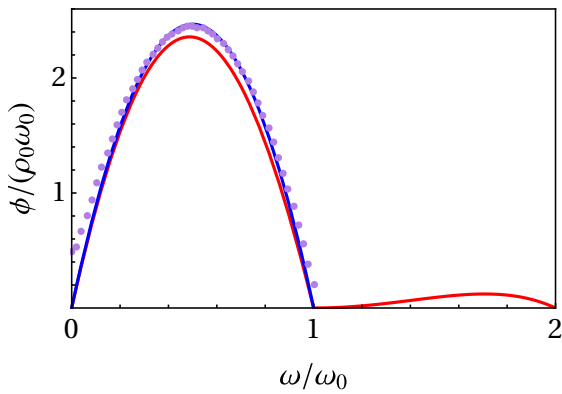


FIG. 2. Normalized spectral photon flux density in the case of CW driving ($\rho_0\omega_0 = C^2|E_0|^2\omega_0^2/\pi^2$). Calculations including up to second (blue) and fourth order (red) terms in $\alpha = dE_0$ have been included. The value of the factor $\pi^4\rho_0\omega_0/4$ governing the smallness of the α^4 term with respect to the α^2 term is 0.02. Although the second order contribution has a parabolic shape in the range of ω/ω_0 from 0 to 1, higher order terms allow for modification of this shape. They also lead to the appearance of photons with frequencies larger than ω_0 and its harmonics. The dotted curve shows the average spectral photon flux density for a measurement over a finite time interval $\Delta t = NT$ with $N = 50$, where $T = 2\pi/\omega_0$ is the period of the driving field.

PDC processes involving light pulses with a well-defined central frequency [13, 35]. Furthermore, the considered phase matching conditions lead to spatially distinguished signal and idler pulses. In contrast, Eqs. (1) and (5) do not rely on the assumption of a bandwidth much smaller than the central frequency. There is also no separation in the propagation direction of the outgoing photons.

Using Eqs. (3) and (5) we calculate perturbatively in d the expectation value of the spectral photon density (SPD) operator, $\hat{\rho}(\omega) = \hat{a}^\dagger(\omega)\hat{a}(\omega)$, for the state $|\{\xi\}_\omega\rangle = \hat{S}[\xi]|0\rangle$ resulting from the pulse-induced squeezing process [36]. It is instructive, however, to begin by analysing continuous wave (CW) driving with frequency ω_0 , $E_{\text{MIR}}(\tau) = E_0e^{-i\omega_0\tau} + E_0^*e^{i\omega_0\tau}$. Due to the infinite duration of the CW field, the SPD diverges for any frequency of interest. In this case, the spectral photon flux density, $\phi(\omega)$, can be defined for a time interval Δt and calculated [36], as is shown in Fig. 2. We see that PDC is maximally probable near the degeneracy point ($\omega \approx \omega_0/2$), while output at the drive frequency ω_0 is absent. Additionally, higher order contributions show that the photons generated by PDC can be upconverted to $3\omega_0/2$ by mixing with the coherent pump field.

Next, we study two cases of the pulsed driving field. Firstly, let us consider an ideal half-cycle pulse (HCP) of light with temporal profile $E_{\text{MIR}}(\tau) = E_0\text{sech}(\Gamma\tau)$ and Fourier transform $E_{\text{MIR}}(\omega) = \frac{E_0}{2\Gamma}\text{sech}(\frac{\pi\omega}{2\Gamma})$ [39]. In this

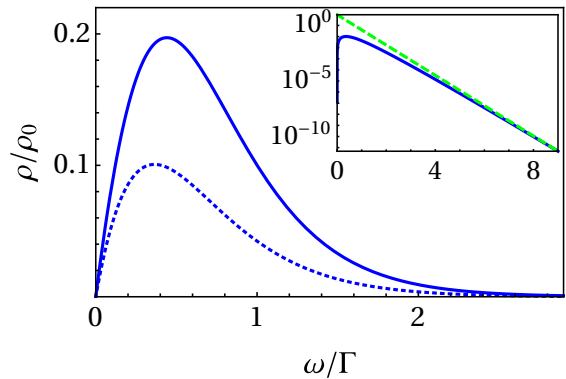


FIG. 3. Normalized spectral photon density (SPD) for the driving HCP (dotted blue) and SCP (solid blue) cases ($\rho_0 = C^2E_0^2\Gamma/\pi^2$) in the leading (α^2) order. The exponential behavior of the spectra can be better analysed in a logarithmic plot, presented for the HCP case in the inset (which has the same high-frequency behavior as for the SCP case). The SPD is shown in blue, while the asymptotic dotted straight line represents a fit of the form $Ae^{-\pi(\omega/\Gamma)}$.

case the SPD, $\rho(\omega) = \langle\{\xi\}_\omega|\hat{\rho}(\omega)|\{\xi\}_\omega\rangle$, reads

$$\rho(\omega) = \frac{C^2E_0^2}{\pi^2}\omega \ln\left(1 + e^{-\frac{\pi\omega}{\Gamma}}\right). \quad (6)$$

For an ideal single-cycle pulse (SCP) of form $E_{\text{MIR}}(\tau) = -E_0(\Gamma\tau)\text{sech}(\Gamma\tau)$, which corresponds to $E_{\text{MIR}}(\omega) = \frac{\pi E_0}{4i\Gamma}\text{sech}(\frac{\pi\omega}{2\Gamma})\tanh(\frac{\pi\omega}{2\Gamma})$ in the frequency domain, we find

$$\rho(\omega) = \frac{C^2E_0^2}{12}\omega \left[\ln\left(1 + e^{-\frac{\pi\omega}{\Gamma}}\right) + \frac{1}{2}\text{sech}^2\left(\frac{\pi\omega}{2\Gamma}\right) \right]. \quad (7)$$

Both Eqs. (6) and (7) show that for high frequencies the SPD falls off as $\exp(-\pi\omega/\Gamma)$, i.e., its exponential decay is determined by the duration of the driving field Γ^{-1} (see Fig. 3).

Electric field variance.—Another insight into the generated quantum field is provided by its normally ordered variance (NOV), $V(\tau)$, which can be calculated as $V(\tau) = \langle\{\xi\}_\omega|:\hat{\Delta}E(\tau):^2|\{\xi\}_\omega\rangle$ since $\langle\{\xi\}_\omega|:\hat{\Delta}E(\tau):|\{\xi\}_\omega\rangle = 0$. Here $:\hat{O}:$ denotes normal ordering for an operator \hat{O} [33]. For the first order term in the squeezing strength $r = |\alpha|\zeta/n$ ($\alpha = dE_0$, $\zeta = \Gamma L/c_0$) we obtain [36]

$$V^{(1)}(\tau) = \frac{\hbar C}{24\pi\epsilon_0 c_0 n A} \frac{\partial^3 E_{\text{MIR}}(\tau)}{\partial \tau^3}. \quad (8)$$

The corresponding second order term, $V^{(2)}(\tau)$, was also calculated (for details, see Ref. [36]). The resulting temporal traces for the three aforementioned shapes of E_{MIR} are shown in Fig. 4 for driving field strengths such that the perturbation approach is still valid but the impact of the second order contribution becomes visible.

The dynamics of the NOV is accessible via quantum electro-optic sampling [16–18] when the time resolution

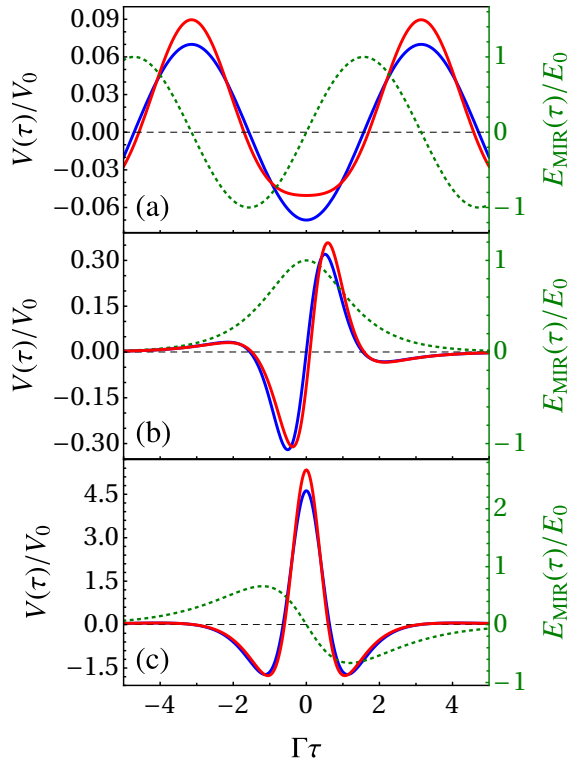


FIG. 4. Dynamics of the normally ordered variance (NOV), $V(\tau)$, of the emitted quantum electric field for (a) CW, (b) HCP and (c) SCP driving (dotted green). Contributions up to the first $V^{(1)}(\tau)$ (blue) and the second $V^{(1)}(\tau) + V^{(2)}(\tau)$ (red) order in the squeezing strength r are shown. The NOV is normalized by $V_0 = \hbar\Gamma^2/(24\pi\epsilon_0 c_0 nA)$, while time is normalized by Γ ($\Gamma = \omega_0$ for CW driving). $r = 0.07$ for (a), 0.21 for (b) and 1.54 for (c).

and sensitivity are high enough [40]. Within the range of validity of our perturbation theory, both the NOV and the SPD are interrelated via the shape of E_{MIR} . This motivates future experiments to retrieve SPD information from the temporal traces of the detected field variance obtained via quantum electro-optic sampling.

Analogue gravity and world lines of light.— The quantum properties of the generated light are determined by the effectively curved space-time that the light modes experience while travelling through the NX, dressed by the input driving field. The metrics of such space-time can be extracted from the dispersion relation for the propagating quantum electric field [41, 42]. This fact allows us to derive the null geodesic equations [43] for the respective modes (for details, see Ref. [36]). The world lines follow the equations

$$\frac{\alpha\zeta}{n} \frac{z}{L} - \sinh \left[\frac{\zeta}{L} (c_0 t - nz) \right] = C_1, \quad (9)$$

$$\frac{\alpha\zeta}{n} \frac{z}{L} + \text{Chi} \left[\left| \frac{\zeta}{L} (c_0 t - nz) \right| \right] = C_2, \quad (10)$$

for the HCP and SCP driving cases, respectively. The

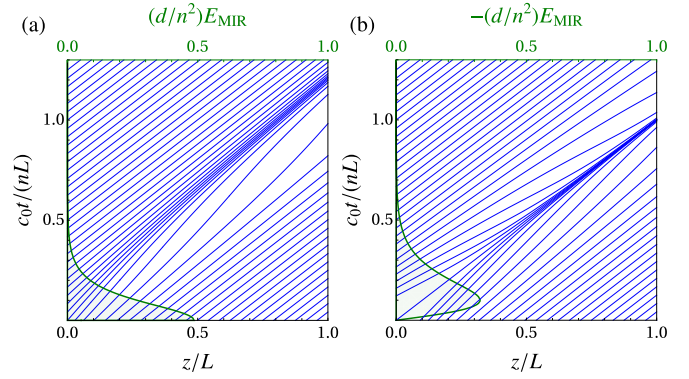


FIG. 5. World lines of the modes of quantum light propagating through the NX for HCP (a) and SCP (b) driving. Each world line (blue) is defined by its initial condition, which is given by a certain event at the boundary of the crystal and correspondingly by the amplitude of the driving field (green) at this event. Here $\alpha/n^2 = 0.49$ and $n\zeta = 12$ (see Ref. [36]).

constants C_1 and C_2 in these equations define the distance of a propagating wave front relative to the center of the driving field at the entrance of the crystal. $\alpha = dE_0$ gives the strength of the nonlinear perturbation, $\zeta = \Gamma L/c_0$ determines the spatial extension of the curvature (i.e. acceleration) relative to the length of the crystal and $\text{Chi}(x)$ is the hyperbolic cosine integral function [44]. The world lines for several values of C_1 and C_2 are shown in Fig. 5 alongside with a projection of the normalized driving fields. The acceleration of the modes is confined to finite regions of space-time. Moreover, the density of world lines projected along a line perpendicular to the light rays $t - nz/c_0 = \tau = \text{const}$ determines the effective change in the flow of time and thereby is connected with the temporal profiles of the detected variance [40], as can be comprehended through comparison between Figs. 4(a,b) and 5(a,b). The evolution of the modes in the space-time curved due to a spatio-temporal varying refractive index leads to the generation of quantum radiation. It is thus insightful to discuss our results in relation to one of the most well-known examples of the creation of quantum light from the vacuum through acceleration: the Unruh-Davies effect.

Unruh-Davies radiation and the diamond temperature.— From Planck's law, the SPD of thermal radiation is dominated by $\exp(-\frac{\hbar\omega}{k_B T})$ at large frequencies, with a decay dependent on the temperature T (k_B is Boltzmann's constant). According to the Unruh-Davies effect [20, 21], for the quantum radiation detected in the reference frame of a uniformly accelerated observer, moving in the vacuum of an inertial observer (Minkowski vacuum), the temperature is given by $T_U = \hbar a/(2\pi k_B c_0)$. Here a is the acceleration measured in the accelerated observer's reference frame.

In the context of an optical analogue of the Unruh-Davies effect, the detector remains at rest while the light

follows an accelerated trajectory within a nonlinear material with time-varying refractive index. If one employs a crystal with $\chi^{(2)}$ nonlinearity as such a material, the refractive index can be modulated by a coherent driving [45] MIR field through the Pockels effect. To lowest order in E_{MIR} the acceleration of the quantum light modes within the crystal depends on its time derivative [24]. From Eqs. (6) and (7), however, it is possible to see that the exponential decay depends only on its duration Γ^{-1} .

Martinetti and Rovelli [29] considered the case of an observer with finite lifetime \mathcal{T} uniformly accelerated in the vacuum of an inertial observer. In this case the Minkowski vacuum is observed as a thermal state with time-dependent temperature

$$T = T_U \varepsilon / [\sqrt{1 + \varepsilon^2} - \sqrt{1 + \varepsilon^2 \tilde{t}^2}], \quad \varepsilon = 2T_U/T_D, \quad (11)$$

where $\tilde{t} = 2t/\mathcal{T} \in (-1, 1)$ is the normalized lab time and $T_D = 2\hbar/(\pi k_B \mathcal{T})$. Since the observer's trajectory lies within a space-time diamond determined by \mathcal{T} , T_D is termed the diamond's temperature. The minimal value T_{min} of T , in the middle of the observer's lifetime, should play the dominant role for the high-frequency tail of the emitted photon spectra. For sufficiently large lifetime or acceleration, $\varepsilon \gg 1$ and T_{min} coincides with the Unruh-Davies temperature T_U . In the opposite situation, $\varepsilon \ll 1$ and $T_{\text{min}} \approx T_D$, given directly by the lifetime of the accelerated observer. This result was reinforced through analysis of a two-level detector model with a properly scaled Hamiltonian, which for a finite measurement time reveals that the detected temperature should be T_D [30].

The analysis of the present work holds when ε is small enough [36]. The spectra of the outgoing quantum light in our analogue optical system should decay as $\exp(-\frac{\hbar\omega}{k_B T})$ with a temperature related to the duration of E_{MIR} , since it dictates the duration of the acceleration of light within the NX. This result is reflected in Eqs. (6) and (7) through the decay dependence on Γ . This can also be seen qualitatively in Fig. 1(b) and Fig. 5, where curved world lines are confined to certain space-time zones. The same does not happen in the case of a CW driving field, since the respective electric field has no defined time duration.

Conclusions.—we propose a generalized squeezing operator to describe ultrabroadband squeezed pulses generated in thin $\chi^{(2)}$ NXs by MIR coherent driving fields. We analyse the spectral properties of these squeezed states for three different shapes of the driving field and connect these results to the time-dependent NOV of the electric field operator. Ultimately, we account for the finite duration of the driving MIR pulses and relate our results to the diamond's temperature in an Unruh-Davies-like effect with a finite lifetime for the observer.

Funding by the DFG within SFB 767 and the Baden-Württemberg Stiftung via the Eliteprogramme for Postdocs (project "Fundamental aspects of relativity and

causality in time-resolved quantum optics") as well as by the LGFG PhD fellowship program and Young Scholar Fund of the University of Konstanz is gratefully acknowledged. The authors thank Dr. Takayuki Kurihara, Prof. Dr. Rudolf Haussmann, Philipp Sulzer, Maximilian Russ and Matthew Brooks for the fruitful and elucidating discussions.

-
- [1] L.-A. Wu, H. J. Kimble, J. L. Hall, and H. Wu, *Phys. Rev. Lett.* **57**, 2520 (1986).
 - [2] P. G. Kwiat, K. Mattle, H. Weinfurter, A. Zeilinger, A. V. Sergienko, and Y. Shih, *Phys. Rev. Lett.* **75**, 4337 (1995).
 - [3] C. M. Caves, *Phys. Rev. D* **23**, 1693 (1981).
 - [4] J. Aasi *et al.*, *Nat. Photonics* **7**, 613 (2013).
 - [5] M. Hillery, *Phys. Rev. A* **61**, 022309 (2000).
 - [6] J. L. O'Brien, A. Furusawa, and J. Vučković, *Nat. Photonics* **3**, 687 (2009).
 - [7] N. Gisin, G. Ribordy, W. Tittel, and H. Zbinden, *Rev. Mod. Phys.* **74**, 145 (2002).
 - [8] M. Xiao, L.-A. Wu, and H. J. Kimble, *Phys. Rev. Lett.* **59**, 278 (1987).
 - [9] V. Giovannetti, S. Lloyd, and L. Maccone, *Science* **306**, 1330 (2004).
 - [10] W. Wasilewski, A. I. Lvovsky, K. Banaszek, and C. Radzewicz, *Phys. Rev. A* **73**, 063819 (2006).
 - [11] K. J. Blow, R. Loudon, S. J. D. Phoenix, and T. J. Shepherd, *Phys. Rev. A* **42**, 4102 (1990).
 - [12] Y. Shaked, R. Pomerantz, R. Z. Vered, and A. Pe'er, *New J. Phys.* **16**, 053012 (2014).
 - [13] A. Christ, B. Brecht, W. Mauerer, and C. Silberhorn, *New J. Phys.* **15**, 053038 (2013).
 - [14] N. A. Ansari and V. I. Man'ko, *Phys. Lett. A* **223**, 31 (1996).
 - [15] V. Ansari, G. Harder, M. Allgaier, B. Brecht, and C. Silberhorn, *Phys. Rev. A* **96**, 063817 (2017).
 - [16] C. Riek, D. V. Seletskiy, A. S. Moskalenko, J. Schmidt, P. Krauspe, S. Eckart, S. Eggert, G. Burkard, and A. Leitenstorfer, *Science* **350**, 420 (2015).
 - [17] A. S. Moskalenko, C. Riek, D. V. Seletskiy, G. Burkard, and A. Leitenstorfer, *Phys. Rev. Lett.* **115**, 263601 (2015).
 - [18] C. Riek, P. Sulzer, M. Seeger, A. S. Moskalenko, G. Burkard, D. V. Seletskiy, and A. Leitenstorfer, *Nature (London)* **541**, 376 (2017).
 - [19] N. D. Birrell, N. D. Birrell, and P. Davies, *Quantum fields in curved space* (Cambridge university press, New York, 1984).
 - [20] W. G. Unruh, *Phys. Rev. D* **14**, 870 (1976).
 - [21] P. C. W. Davies, *J. Phys. A: Math. Gen.* **8**, 609 (1975).
 - [22] S. W. Hawking, *Comm. Math. Phys.* **43**, 199 (1975).
 - [23] E. Yablonovitch, *Phys. Rev. Lett.* **62**, 1742 (1989).
 - [24] T. G. Philbin, C. Kuklewicz, S. Robertson, S. Hill, F. König, and U. Leonhardt, *Science* **319**, 1367 (2008).
 - [25] F. Belgiorno, S. L. Cacciatori, M. Clerici, V. Gorini, G. Ortenzi, L. Rizzi, E. Rubino, V. G. Sala, and D. Faccio, *Phys. Rev. Lett.* **105**, 203901 (2010).
 - [26] F. Belgiorno, S. L. Cacciatori, G. Ortenzi, L. Rizzi, V. Gorini, and D. Faccio, *Phys. Rev. D* **83**, 024015

- (2011).
- [27] M. F. Linder, R. Schützhold, and W. G. Unruh, *Phys. Rev. D* **93**, 104010 (2016).
- [28] P. Chen and G. Mourou, *Phys. Rev. Lett.* **118**, 045001 (2017).
- [29] P. Martinetti and C. Rovelli, *Class. Quantum Gravity* **20**, 4919 (2003).
- [30] D. Su and T. C. Ralph, *Phys. Rev. D* **93**, 044023 (2016).
- [31] C. F. Lo and R. Sollie, *Phys. Rev. A* **47**, 733 (1993).
- [32] M. F. Maghrebi, R. Golestanian, and M. Kardar, *Phys. Rev. A* **88**, 042509 (2013).
- [33] W. Vogel and D. Welsch, *Quantum Optics* (Wiley, Weinheim, 2006).
- [34] R. Loudon, *The Quantum Theory of Light* (Oxford University Press, New York, 2000).
- [35] K. E. Dorfman, F. Schlawin, and S. Mukamel, *Rev. Mod. Phys.* **88**, 045008 (2016).
- [36] See Supplemental Material at [URL will be inserted by publisher] for details.
- [37] K. S. Thorne and R. D. Blandford, *Modern Classical Physics: Optics, Fluids, Plasmas, Elasticity, Relativity, and Statistical Physics* (Princeton University Press, Princeton, 2017).
- [38] V. A. De Lorenci and R. Klippert, *Phys. Rev. D* **65**, 064027 (2002).
- [39] A. S. Moskalenko, Z.-G. Zhu, and J. Berakdar, *Phys. Rep.* **672**, 1 (2017).
- [40] M. Kizmann, T. L. M. Guedes, D. V. Seletskiy, A. S. Moskalenko, A. Leitenstorfer, and G. Burkard, arXiv:1807.10519.
- [41] M. Novello, V. A. De Lorenci, J. M. Salim, and R. Klippert, *Phys. Rev. D* **61**, 045001 (2000).
- [42] U. Leonhardt and P. Piwnicki, *Phys. Rev. A* **60**, 4301 (1999).
- [43] B. Schutz, *A first course in general relativity* (Cambridge University Press, New York, 2009).
- [44] I. S. Gradshteyn and I. M. Ryzhik, *Table of integrals, series, and products* (Academic press, San Diego, 2014).
- [45] R. J. Glauber, *Phys. Rev.* **131**, 2766 (1963)

Supplemental Material

Spectra of ultrabroadband squeezed pulses and the finite-time Unruh-Davies effect

T.L.M. Guedes, M. Kizmann, D.V. Seletskiy, A. Leitenstorfer, G. Burkard and A.S. Moskalenko

1. SPECTRAL PHOTON DENSITY AND SPECTRAL PHOTON FLUX DENSITY

Using the expressions for the transformed creation and annihilation operators defined by Eqs. (3) and (5) we calculate up to second order in d the expectation value of the operator $\hat{a}^\dagger(\omega)\hat{a}(\omega')$ for the states $|\{\xi\}_\omega\rangle = \hat{S}[\xi]|0\rangle$ resulting after the squeezing process,

$$\begin{aligned} \langle\{\xi\}_\omega|\hat{a}^\dagger(\omega)\hat{a}(\omega')|\{\xi\}_\omega\rangle &= \theta(-\omega)\theta(-\omega')\delta(\omega-\omega') - iC\Theta_-(-\omega, -\omega')E_{\text{MIR}}(\omega'-\omega) \\ &- \frac{C^2}{2}\Theta_+(-\omega, -\omega')\int_{-\infty}^{\infty}d\tilde{\omega}\tilde{\omega}E_{\text{MIR}}^*(\omega+\tilde{\omega})E_{\text{MIR}}(\tilde{\omega}+\omega') + C^2\sqrt{|\omega\omega'|}\int_{-\infty}^{\infty}d\tilde{\omega}\tilde{\omega}E_{\text{MIR}}^*(\omega+\tilde{\omega})E_{\text{MIR}}(\tilde{\omega}+\omega'), \end{aligned} \quad (\text{S1})$$

where $\Theta_\pm(\omega, \omega') = \sqrt{|\omega\omega'|}[\theta(\omega)\text{sign}(\omega) \pm \theta(\omega')\text{sign}(\omega')]$. The spectral photon density, $\rho(\omega)$, is defined from Eq. (S1) by setting $\omega = \omega' > 0$.

In order to circumvent the problem of the diverging spectral photon density in the case of the CW driving, we can use a different set of creation and annihilation operators [S1, pp. 187-191] for a finite observation time Δt . For $\mu \in \mathbb{Z}^+$ we define $\hat{a}_\mu = -i\sqrt{\frac{4\pi\epsilon c_0 A}{\hbar\omega_\mu\Delta t}}\int_0^{\Delta t}dt\delta\hat{E}^{(+)}(z, t)\exp(i\omega_\mu\tau)$, with $\omega_\mu = 2\pi\mu/\Delta t$, $\delta\hat{E}^{(+)}(z, t) = \int_0^\infty d\omega\delta\hat{E}(z; \omega)\exp(-i\omega\tau)$ and $\Delta t = NT$ [T is the period of $E_{\text{MIR}}(\tau)$ and $\tau = t - nz/c_0$ is the retarded time]. The larger the number N of periods observed, the higher the frequency resolution. The photon number in mode μ reads $\langle\hat{n}_\mu\rangle = C^2|E_0|^2\frac{\Delta t}{\omega_\mu}\int_0^{\omega_0}d\omega\omega^2(\omega_0 - \omega)\text{sinc}^2[\frac{\pi N}{\omega_0}(\omega_\mu - \omega)]$ for $\omega \in (0, \omega_0)$. Dividing $\langle\hat{n}_\mu\rangle$ by $\Delta t\Delta\omega$ ($\Delta\omega = \omega_0/N$), we obtain the time-averaged spectral photon flux density measured over the time interval Δt , $\langle\hat{\phi}_\mu\rangle$. In the limit of $N \rightarrow \infty$ this expression is exactly the function multiplying the delta function in Eq. (S1) for CW driving when $\omega' \rightarrow \omega$. The limiting spectral photon flux density (the average distribution of generated photons in the frequency domain per unit of time and frequency) including terms up to the fourth order in $\alpha = dE_0$ reads:

$$\begin{aligned} \phi(\omega) \equiv \langle\hat{\phi}(\omega)\rangle &= C^2|E_0|^2\omega(\omega_0 - \omega)\theta(\omega_0 - \omega) + \frac{C^4}{4}|E_0|^4\theta(2\omega_0 - \omega)\omega(2\omega_0 - \omega)(\omega_0 - \omega)^2 \\ &+ \frac{C^4}{3}|E_0|^4\theta(\omega_0 - \omega)\omega(3\omega^3 - 6\omega_0\omega^2 + 5\omega_0^2\omega - 2\omega_0^3). \end{aligned} \quad (\text{S2})$$

2. CONVERGENCE OF THE PERTURBATIVE EXPANSION, HIGH-FREQUENCY TAIL AND ROLE OF THE PULSE SHAPE

The validity of restricting our calculations of the spectral photon density to second order terms can be verified by analysing the structure of higher order terms in $\rho(\omega)$ ($\omega > 0$):

$$\begin{aligned} \rho(\omega) &= C^2\int_0^\infty d\omega'\omega\omega'|E(\omega+\omega')|^2 - C^3\Re\left\{i\int_{-\infty}^\infty d\omega'\int_0^\infty d\omega''\text{sign}(\omega')|\omega\omega'\omega''|E^*(\omega+\omega'')E(\omega+\omega')E^*(\omega''-\omega')\right\} \\ &+ \frac{1}{3}C^4\Re\left\{\int_{-\infty}^\infty d\omega'd\omega''\int_0^\infty d\omega'''\text{sign}(\omega'\omega'')|\omega\omega'\omega''\omega'''|E^*(\omega+\omega''')E(\omega+\omega')E^*(\omega'-\omega'')E(\omega''+\omega''')\right\} \\ &+ \frac{1}{4}C^4\int_{-\infty}^\infty d\omega'd\omega''\int_0^\infty d\omega'''\text{sign}(\omega'\omega'')|\omega\omega'\omega''\omega'''|E^*(\omega+\omega')E(\omega'-\omega''')E(\omega+\omega'')E^*(\omega''-\omega''') + \dots \end{aligned} \quad (\text{S3})$$

Firstly, we have to answer the question of applicability of the perturbative expansion, in general. Let us consider an ultrashort driving pulse of a single-cycle or subsycle shape and duration $\mathcal{T} = 1/\Gamma'$. Normalizing in Eq. (S3) frequencies by Γ' and Fourier components of the electric field by E_0/Γ' , from the structure of expansion (S3) we see that it holds only if the condition

$$|CE_0|\Gamma' \sim \varepsilon\frac{L}{L_p} \ll 1 \quad (\text{S4})$$

is fulfilled. Here we used the definitions for C and $\varepsilon = T_U/T_D$ from the main text. L is the crystal length and $L_p \sim c_0/\Gamma'$ is the spatial extent of the driving pulse. Notice that in comparison to the condition separating the two regimes in Eq. (11) an additional factor L/L_p appears in Eq. (S4). This is caused by the different spatial regions giving rise to detected photons in the situation described by Martinetti and Rovelli and in our analogue case.

Now let us consider the regime when Eq. (S4) is valid and the perturbation expansion is applicable. We want to analyze the spectral photon density at $\omega \gg \Gamma'$. Does the inclusion solely of the lowest order term ($\propto C^2$) of the expansion capture the correct high-frequency behavior of the spectral photon density in the high-frequency tail? It turns out that the answer depends on the shape of the pulse. A clear indication that the lowest order term is not always sufficient for the studied question is provided immediately by the results demonstrated for the case of CW driving, cf. Eq. (S2) and Fig. 2. The contribution of the C^2 term is limited in the frequency domain by the driving frequency ω_0 . The frequency conversion processes leading to C^{2n} terms ($n > 1$) extend the frequency range for the photon observation to $n\omega_0$. Thus however small C might be, in the case of the CW driving, it is necessary to include the terms of sufficiently large order if high frequencies are considered. The resulting values of the density decay rapidly with the frequency increase but these small values are dominated by the contributions of higher and higher order.

The Fourier transforms of the considered pulsed fields $E(\omega)$ are confined to the frequency range $-\Gamma' < \omega < \Gamma'$, declining rapidly outside of this range. Considering the contributions of C^{2n} terms to the high-frequency tail of the spectral photon density $\rho(\omega)$, there are two competing effects which have to be taken into account: (i) the decay behavior of $E(\omega)$ with ω and (ii) the increase of the maximum value ω_n^{\max} of ω such that the frequencies ω_i of all fields $E(\omega_i)$ ($i = 1, \dots, n$) in the corresponding integrands $E(\omega_1) \dots E(\omega_n)$ do not leave the interval $(-\Gamma', \Gamma')$. One can see that there are always terms of the order C^{2n} such that $\omega_n^{\max} = n\Gamma'$. For $\omega \in (0, n\Gamma')$ the resulting contribution from these terms does not decay rapidly with increase of frequency. Without loss of generality, the odd order C^{2n+1} terms can be excluded from the current discussion since their extension in ω is also limited by $\omega_{\max} = n\Gamma'$. With respect to C^{2n} terms, the contribution from $C^{2(n+1)}$ terms extends further in frequency by Γ' to $\omega_{\max} = (n+1)\Gamma'$ but scales down with factor $|CE_0|\Gamma'$.

We want to compare the impact of the effects (i) and (ii) for the high-frequency tail of $\rho(\omega)$. The decay due to (ii) is roughly independent of the pulse shape and is given by $\sim \exp(-\omega/\gamma)$, where the inverse decay constant γ can be estimated as $\gamma = \ln[1/(|CE_0|\Gamma')] \Gamma'/2$. Notice that in the considered regime the value of the logarithm is positive. In contrast, the character of the decay due to (i) is determined by the pulse shape. In the case when $E(\omega)$ decays as $\exp(-\omega/\Gamma')$, as for the pulse shapes considered in the main text, the lowest order C^2 term declines as $\exp(-2\omega/\Gamma')$ for $\omega \gg \Gamma'$. The inverse decay rate $\Gamma'/2$ is lower than γ if Eq. (S4) is well fulfilled. Then it is sufficient to include only the C^2 term for the study of the high frequency tail of the photon density. The situation is different, if $E(\omega)$ vanishes super-exponentially with increasing frequency. For example, Gaussian pulses in the time domain have the Gaussian shape also in the frequency domain and decay as $\exp(-\omega^2/\Gamma'^2)$. For them the effect (ii) would always dominate at high enough frequencies. Higher order contributions must be included for an appropriate description. One can still expect a decay close to exponential, with the inverse decay constant $\sim \gamma$. Notice that if $|CE_0|\Gamma'$ is not too small, which is anyway required in order to avoid having too few photons for detection, γ does not deviate much from Γ' and remains mainly determined by the pulse duration.

3. NORMALLY ORDERED ELECTRIC FIELD VARIANCE

Let us now introduce a continuous frequency-dependent quadrature operator $\hat{x}(\omega, \phi)$ for the generated quantum electric field

$$\delta \hat{E}(t, z) = \int_0^\infty d\omega \sqrt{\frac{\hbar\omega}{4\pi\epsilon c_0 n A}} \hat{x}(\omega, \phi), \quad (\text{S5})$$

where $\hat{x}(\omega, \phi) = \hat{a}(\omega)e^{i\phi(\omega, t, z)} + \hat{a}^\dagger(\omega)e^{-i\phi(\omega, t, z)}$ and $\phi(\omega, t, z) = -\omega(t - nz/c_0) + \pi/2$. Equation (S5) enables us to connect the normally ordered variance of $\hat{x}(\omega, \phi)$ to the time-dependent normally ordered variance of the electric field operator. From equation (S5) we see that the normally ordered variance $\langle :[\delta \hat{E}(\tau)]^2: \rangle$ depends on the values of $\langle : \hat{x}(\omega) : \rangle$ and $\langle : \hat{x}(\omega) \hat{x}(\omega') : \rangle$. For the state $|\{\xi\}_\omega\rangle$, $\langle \{\xi\}_\omega | \hat{x}(\omega) | \{\xi\}_\omega \rangle = \langle 0 | \hat{S}^\dagger \hat{x}(\omega) \hat{S} | 0 \rangle$ whereas $\hat{S}^\dagger \hat{x}(\omega) \hat{S}$ is linear in both $\hat{a}(\omega)$ and $\hat{a}^\dagger(\omega)$, resulting in a zero expectation value. The other expectation value reads

$$\begin{aligned} \langle \{\xi\}_\omega | : \hat{x}(\omega) \hat{x}(\omega') : | \{\xi\}_\omega \rangle &= \langle \{\xi\}_\omega | \hat{a}(\omega)^\dagger \hat{a}(\omega') | \{\xi\}_\omega \rangle e^{-i(\phi - \phi')} + \langle \{\xi\}_\omega | \hat{a}^\dagger(\omega') \hat{a}(\omega) | \{\xi\}_\omega \rangle e^{i(\phi - \phi')} \\ &+ \langle \{\xi\}_\omega | \hat{a}(\omega) \hat{a}(\omega') | \{\xi\}_\omega \rangle e^{i(\phi + \phi')} + \langle \{\xi\}_\omega | \hat{a}^\dagger(\omega) \hat{a}^\dagger(\omega') | \{\xi\}_\omega \rangle e^{-i(\phi + \phi')}. \end{aligned} \quad (\text{S6})$$

The four terms in (S6) can be calculated by transforming the creation and annihilation operators with the squeezing operator as in Eq. (3) and taking the vacuum expectation value, Eq. (S1). The normally ordered variance thus reads

$$\langle \{\xi\}_\omega | : [\delta \hat{E}(\tau)]^2 : | \{\xi\}_\omega \rangle = \langle \{\xi\}_\omega | : [\delta \hat{E}(\tau)]^2 : | \{\xi\}_\omega \rangle^{(1)} + \langle \{\xi\}_\omega | : [\delta \hat{E}(\tau)]^2 : | \{\xi\}_\omega \rangle^{(2)} = V^{(1)}(\tau) + V^{(2)}(\tau), \quad (\text{S7})$$

where

$$\langle \{\xi\}_\omega | : [\delta \hat{E}(\tau)]^2 : | \{\xi\}_\omega \rangle^{(1)} = \frac{\hbar C}{2\pi\epsilon_0 c_0 A} \int_0^\infty d\omega d\omega' |\omega\omega'| \Im [E_{\text{MIR}}(\omega + \omega') e^{-i(\omega + \omega')\tau}] = \frac{\hbar C}{24\pi\epsilon_0 c_0 n A} \frac{\partial^3 E_{\text{MIR}}(\tau)}{\partial \tau^3}, \quad (\text{S8})$$

and

$$\langle \{\xi\}_\omega | : [\delta \hat{E}(\tau)]^2 : | \{\xi\}_\omega \rangle^{(2)} = \frac{\hbar C^2}{2\pi\epsilon_0 c_0 n A} \sum_{i=1,2,3} V_i^{(2)}(\tau), \quad (\text{S9})$$

with

$$V_1^{(2)} = \int_0^\infty d\omega \int_0^\infty d\omega' |\omega\omega'| \int_0^\infty d\omega'' |\omega''| \Re [E_{\text{MIR}}^*(\omega + \omega'') E_{\text{MIR}}(\omega'' + \omega') e^{i(\omega - \omega')\tau}], \quad (\text{S10})$$

$$V_2^{(2)} = \frac{1}{2} \int_0^\infty d\omega \int_0^\infty d\omega' |\omega\omega'| \int_{-\infty}^\infty d\omega'' \omega'' \Re [E_{\text{MIR}}(\omega + \omega'') E_{\text{MIR}}^*(\omega'' - \omega') e^{-i(\omega + \omega')\tau}], \quad (\text{S11})$$

$$V_3^{(2)} = - \int_0^\infty d\omega \int_0^\infty d\omega' |\omega\omega'| \int_0^\infty d\omega'' |\omega''| \Re [E_{\text{MIR}}(\omega - \omega'') E_{\text{MIR}}(\omega'' + \omega') e^{-i(\omega + \omega')\tau}]. \quad (\text{S12})$$

Depending on the shape of E_{MIR} , expressions (S10), (S11) and (S12) can be evaluated either analytically or numerically.

4. WORLD LINE OF A PROPAGATING ELECTRIC FIELD MODE IN A $\chi^{(2)}$ NONLINEAR CRYSTAL

We start with the wave equation

$$\frac{\partial^2 \delta \hat{E}(z, t)}{\partial z^2} - \frac{n^2}{c_0^2} \frac{\partial^2 \delta \hat{E}(z, t)}{\partial t^2} = \frac{1}{c_0^2} \frac{\partial^2}{\partial t^2} [dE_{\text{MIR}}(z, t) \delta \hat{E}(z, t)] \quad (\text{S13})$$

for the propagation of the vacuum electric field operator within a crystal with refractive index modulated by the MIR coherent field (E_{MIR}). Considering that $\langle 0 | \delta \hat{E} | 0 \rangle = 0$, we use an eikonal approximation to write the electric field operator as [S2]

$$\delta \hat{E}(z, t) = \hat{A}(z, t) e^{i\phi(z, t)}, \quad (\text{S14})$$

where the phase ϕ changes in space and time much faster than \hat{A} . Following the eikonal approximation we define the wave vector and angular frequency fields by

$$k(z, t) \equiv \nabla \phi(z, t) \quad \text{and} \quad \omega(z, t) \equiv -\partial_t \phi(z, t). \quad (\text{S15})$$

Inserting Eq. (S14) into Eq. (S13) and considering that terms that scale as different powers of k (and/or ω) should vanish independently [S2], we get from the term scaling as k^2 the following dispersion relation:

$$k^2(z, t) - \left[\frac{n^2}{c_0^2} + \frac{dE_{\text{MIR}}(z, t)}{c_0^2} \right] \omega^2(z, t) = 0. \quad (\text{S16})$$

Relation (S16) gives an analogue of the classical Hamiltonian, $H \propto \omega(k, z, t)$, from which the Hamilton equations can be defined considering k to be independent of z . From Eqs. (S14) and (S13) the term scaling as k gives

$$\frac{d\hat{A}(z, t)}{d\tau^0} = \frac{\partial \hat{A}(z, t)}{\partial t} + \frac{\omega}{k} \frac{\partial \hat{A}(z, t)}{\partial z} = - \left(\frac{d\omega^2}{c_0^2 k} \right) \frac{\partial E_{\text{MIR}}(z, t)}{\partial t} \hat{A}. \quad (\text{S17})$$

In expression (S17) $d/d\tau^0$ is the derivative with respect to the proper time ($d/d\tau^0 \equiv u^\alpha \partial_\alpha$, with u^α being the 4-velocity, here with two components only). We see that the amplitude operator propagates along a world line with group velocity $v_g \approx \omega/k$.

Considering relation (S16) and its similarity to the light-cone equation $g^{\mu\nu} K_\mu K_\nu = 0$ for $K_\mu = (\omega/c_0, -k)$, we can derive the metrics [S3]

$$g^{\mu\nu} = \eta^{\mu\nu} + c_0^{-2} u^\mu u^\nu h(z, t), \quad (\text{S18})$$

where

$$h(z, t) = -1 + n^2 + dE_{\text{MIR}}(z, t),$$

$\eta^{\mu\nu} = \text{diag}(1, -1)$ and $u^\mu = \delta_0^\mu c_0$ is the 4-velocity in the momentarily co-moving reference frame. Differentiation of the dispersion relation by $\partial_\lambda = (c_0^{-1} \partial_t, \partial_z)$ reads

$$\partial_\lambda (g^{\mu\nu} K_\mu K_\nu) = g^{\mu\nu}_{;\lambda} K_\mu K_\nu + 2g^{\mu\nu} K_{\mu,\lambda} K_\nu = 0, \quad (\text{S19})$$

where $x^{\mu\nu\dots\zeta}_{;\lambda} \equiv \partial_\lambda x^{\mu\nu\dots\zeta}$.

Following the definition of the Christoffel symbol [S4]

$$\Gamma_{\beta\mu}^\gamma = \frac{1}{2} g^{\alpha\gamma} (g_{\alpha\beta,\mu} + g_{\alpha\mu,\beta} - g_{\beta\mu,\alpha}), \quad (\text{S20})$$

and knowing that the inverse of the metrics is given by

$$g_{\mu\nu} = \eta_{\mu\nu} - c_0^{-2} u_\mu u_\nu \frac{h}{1+h}, \quad (\text{S21})$$

we arrive at the result:

$$\Gamma_{\beta\mu}^\gamma = \frac{1}{2c_0^2(1+h)^2} \left[-u^\gamma u_\beta \partial_\mu h - u^\gamma u_\mu \partial_\beta h + u_\beta u_\mu \eta^{\gamma\alpha} \partial_\alpha h + h u^\gamma \left(-u_\beta \partial_\mu h - u_\mu \partial_\beta h + c_0^{-1} u_\beta u_\mu \partial_0 h \right) \right]. \quad (\text{S22})$$

From equations (S20) and (S22) we explicitly see the symmetry $\Gamma_{\beta\mu}^\gamma = \Gamma_{\mu\beta}^\gamma$.

Since $K_{\mu,\nu} = K_{\nu,\mu}$ ($K_\mu = -\partial_\mu \phi$) and $g^{\mu\nu} K_{\mu,\lambda} = K_{,\lambda}^\nu = K_{\lambda}^\nu$, the covariant derivative of the metrics reads

$$g_{;\lambda}^{\mu\nu} \equiv g_{,\lambda}^{\mu\nu} + \Gamma_{\alpha\lambda}^\mu g^{\alpha\nu} + \Gamma_{\alpha\lambda}^\nu g^{\mu\alpha} = 0, \quad (\text{S23})$$

from which we find that

$$g_{,\lambda}^{\mu\nu} = -\left(\Gamma_{\alpha\lambda}^\mu g^{\alpha\nu} + \Gamma_{\alpha\lambda}^\nu g^{\mu\alpha} \right). \quad (\text{S24})$$

With the help of Eq. (S24) it is easy to show that Eq. (S19) can be rewritten as $K^\mu K_{;\mu}^\lambda = 0$, where $K_{;\mu}^\lambda = K_{,\mu}^\lambda + K^\nu \Gamma_{\nu\mu}^\lambda$ is the covariant derivative of K^λ . Since $K^\mu = g^{\mu\nu} K_\nu = -g^{\mu\nu} \partial_\nu \phi \propto dx^\mu / d\tau^0$ [S5], the relations $K^\mu K_{;\mu}^\lambda = 0$ give the null geodesic equations

$$\frac{d^2 x^\alpha}{d(\tau^0)^2} + \Gamma_{\mu\beta}^\alpha \frac{dx^\mu}{d\tau^0} \frac{dx^\beta}{d\tau^0} = 0, \quad (\text{S25})$$

the components of which can be explicitly written as:

$$\frac{d^2 x^0}{d(\tau^0)^2} + \frac{1}{1+h} \left[-\frac{1}{2} \partial_0 h \left(\frac{dx^0}{d\tau^0} \right)^2 - \partial_1 h \frac{dx^0}{d\tau^0} \frac{dx^1}{d\tau^0} \right] = 0, \quad (\text{S26})$$

$$\frac{d^2 x^1}{d(\tau^0)^2} - \frac{1}{2(1+h)^2} \partial_1 h \left(\frac{dx^0}{d\tau^0} \right)^2 = 0. \quad (\text{S27})$$

In the simple case when $h = n^2 - 1$ (no driving field), equations (S26) and (S27) give straight lines of the form $x^1 = Ax^0 + B$, with A and B defined by the initial conditions (which of course should assure that A will give the correct speed of light within the medium).

Now lets try the case when $h = n^2 - 1 + dE_0 \text{sech}[\frac{\Gamma}{c_0}(x^0 - nx^1)] = n^2 - 1 + \alpha \text{sech}[\zeta(x_L^0 - nx_L^1)]$ (with $x_L^\mu = x^\mu/L$), which correspond to a half-cycle driving field. The geodesic equations read:

$$\left(n^2 + \alpha \text{sech}[\zeta(x_L^0 - nx_L^1)]\right) \frac{d^2 x_L^0}{d(\tau^0)^2} + \alpha \zeta \text{sech}[\zeta(x_L^0 - nx_L^1)] \tanh[\zeta(x_L^0 - nx_L^1)] \left[\frac{1}{2} \left(\frac{dx_L^0}{d\tau^0}\right)^2 - n \frac{dx_L^0}{d\tau^0} \frac{dx_L^1}{d\tau^0} \right] = 0, \quad (\text{S28})$$

$$2 \left(n^2 + \alpha \text{sech}[\zeta(x_L^0 - nx_L^1)]\right)^2 \frac{d^2 x_L^1}{d(\tau^0)^2} - \alpha \zeta n \text{sech}[\zeta(x_L^0 - nx_L^1)] \tanh[\zeta(x_L^0 - nx_L^1)] \left(\frac{dx_L^0}{d\tau^0}\right)^2 = 0. \quad (\text{S29})$$

Knowing that the affine parameter τ^0 parametrizes the world line in the x^0 - x^1 space [i.e. (1+1) space-time] and that the trajectory of the light is supposed to be still time-like within the crystal, we introduce the ansatz: $x_L^1(\tau^0) = f(x_L^0(\tau^0))$. This reduces Eqs. (S28) and (S29) to:

$$\frac{df}{dx_L^0} - \frac{n}{n^2 + \alpha \text{sech}[\zeta(x_L^0 - nf)]} = 0, \quad (\text{S30})$$

$$n \frac{d^2 x_L^0}{d(\tau^0)^2} + \alpha \zeta \text{sech}[\zeta(x_L^0 - nf)] \tanh[\zeta(x_L^0 - nf)] \frac{df}{dx_L^0} \left(\frac{1}{2} - n \frac{df}{dx_L^0}\right) \left(\frac{dx_L^0}{d\tau^0}\right)^2 = 0. \quad (\text{S31})$$

The implicit solution of Eq. (S30) is

$$\alpha x_L^1 - \frac{n}{\zeta} \sinh(\zeta(x_L^0 - nx_L^1)) = C', \quad (\text{S32})$$

where C' is a constant. Equation (S32) gives the approximate world line of the quantum modes within the nonlinear crystal. For the initial condition $x_L^1(0) = 0$, $x_L^0 = l$, we get $C' = -\frac{n}{\zeta} \sinh(\zeta l)$. From expression (S32) we see that in the limit $\alpha \rightarrow 0$ (no refractive index modulation), the solutions are straight lines of the form $nx_L^1 = x_L^0 - l$, i.e. a ray of speed c_0/n . For $\zeta \rightarrow 0$ (constant refractive index modulation), we get $(n + \alpha/n)x_L^1 = x_L^0 - l$, once again straight lines, but with a different speed, as expected. Eq. (S32) can be rewritten as $x_L^0(x_L^1) = nx_L^1 + \zeta^{-1} \sinh^{-1}(\alpha \zeta x_L^1/n + \sinh(\zeta l))$, which gives time as a function of the space coordinate. This same curve has been attained by treating the evolution of the electric field operator in Eq. (S13) with the method of characteristics within the slow varying amplitude approximation [S6]. This means that the characteristic lines leading to the variance profiles of the electric field are also the world lines for the modes of the respective field.

Proceeding in a similar way for $h = n^2 - 1 + dE_0[\Gamma(x^0 - nx^1)] \text{sech}[\frac{\Gamma}{c_0}(x^0 - nx^1)] = n^2 - 1 + \alpha \zeta(x_L^0 - nx_L^1) \text{sech}[\zeta(x_L^0 - nx_L^1)]$, we arrive at the result:

$$\alpha \frac{z}{L} + \frac{n}{\zeta} \text{Chi} \left[\left| \frac{\zeta}{L} (c_0 t - nz) \right| \right] = C''. \quad (\text{S33})$$

Eq. (S33) has similar limiting cases as the example above discussed.

-
- [S1] W. Vogel and D. Welsch, *Quantum Optics* (Wiley, Weinheim, 2006).
[S2] K. S. Thorne and R. D. Blandford, *Modern Classical Physics: Optics, Fluids, Plasmas, Elasticity, Relativity, and Statistical Physics* (Princeton University Press, Princeton, 2017).
[S3] V. A. De Lorenci and R. Klippert, Phys. Rev. D **65**, 064027 (2002).
[S4] B. Schutz, *A first course in general relativity* (Cambridge University Press, New York, 2009).
[S5] U. Leonhardt and P. Piwnicki, Phys. Rev. A **60**, 4301 (1999).
[S6] M. Kizmann *et al.*, arXiv:1807.10519.